

Controlled Li doping of Si nanowires by electrochemical insertion method

G. W. Zhou^{a)}

Beijing Laboratory of Electron Microscopy, Center for Condensed Matter Physics, Chinese Academy of Sciences, Beijing 100080, China

H. Li

Laboratory for Solid State Ionics, Institute of Physics, Chinese Academy of Sciences, Beijing 100080, China

H. P. Sun

Beijing Laboratory of Electron Microscopy, Center for Condensed Matter Physics, Chinese Academy of Sciences, Beijing 100080, China

D. P. Yu

Department of Physics, National Key Laboratory of Mesoscopic Physics, Peking University, Beijing 100871, China

Y. Q. Wang

Beijing Laboratory of Electron Microscopy, Center for Condensed Matter Physics, Chinese Academy of Sciences, Beijing 100080, China

X. J. Huang and L. Q. Chen

Laboratory for Solid State Ionics, Institute of Physics, Chinese Academy of Sciences, Beijing 100080, China

Z. Zhang

Beijing Laboratory of Electron Microscopy, Center for Condensed Matter Physics, Chinese Academy of Sciences, Beijing 100080, China

(Received 22 April 1999; accepted for publication 26 August 1999)

Si nanowires (NWs) were doped with large amounts of Li⁺ ions by an electrochemical insertion method at room temperature. Si NWs with different doping levels were obtained by controlling the discharging/charging of Li/Si NWs cell. The microstructures of Si NWs with different doses of Li⁺ ions were investigated by high-resolution electron microscopy. The crystalline structure of the Si NWs was destroyed gradually with the increasing of Li⁺ ion dose. When the Li⁺ ions were extracted from the amorphous Li-doped Si NWs by the same electrochemical method, local ordering of atoms occurred and recrystallization was observed. The photoluminescence peak and intensity of Li⁺-doped Si NWs are closely related to the doping dose. © 1999 American Institute of Physics. [S0003-6951(99)04842-1]

The recent synthesis of Si nanowires (NWs) (Ref. 1) has stimulated intensive interest in their physical properties and potential application because of their low dimensionality and quantum-confinement effect.² However, controlled doping of Si NWs is a prerequisite for the realization and efficiency of many Si NW-based devices. The properties of these nanostructured materials will be modified by doping large amounts of guest ions.³ Conventional doping techniques have some difficulties in doping Si NWs, especially for controlled doping. Here, we present an electrochemical insertion method to dope Si NWs with Li⁺ ions, and the doping level of the Si NWs can be controlled efficiently by this method. In our work, four Si NW samples with different doping levels were used to study the structural evolution and photoluminescence.

Si NWs samples at different Li⁺ ions insertion/extraction levels were prepared by galvanostatically discharging/charging the typical two-electrode cell, which is composed of a metal lithium foil as a counter electrode, and Si NWs as the other working electrode. Si NWs with different doping levels were obtained by controlling the discharging/charging of the Li/Si NW cells to different volt-

ages. Si NW anodes for transmission electron microscopy investigation were taken out from the cells after electrochemical treatments and sealed in a glass tube containing anhydrous benzene in an argon-filled glove box. A high-resolution electron microscopy (HREM) investigation was conducted using a JEM 2010 microscope operating at 200 kV. Electron energy-loss spectroscopic analysis was carried out by a Philips CM200 FEG microscope equipped with a Gatan parallel electron-loss spectrometer (PEELS).

The morphological characteristics and microstructural aspects of Si NWs were reported in our previous works.^{4,5} The selected area electron diffraction (SAED) patterns of Si NWs at different doping levels are shown in Fig. 1. The SAED pattern in Fig. 1(a) is taken from the undoped Si NWs, and the sharp diffraction rings reveal the *c*-Si structure. Figure 1(b) is taken from Si NWs with a light doping level, which shows two different diffraction patterns. The diffraction pattern in Fig. 1(b) (1) can be indexed with the *c*-Si structure. In Fig. 1(b) (2), the interplanar spacings of the first, second, and third rings are 0.245, 0.212, and 0.151 nm, respectively. These spacings are not consistent with the known Li-Si alloys which can be formed electrochemically only at 415 °C or elevated temperature.⁶ With the increasing dose of Li⁺ ions, only the weak diffraction pattern of the

^{a)}Electronic mail: gwzhou@image.blem.ac.cn

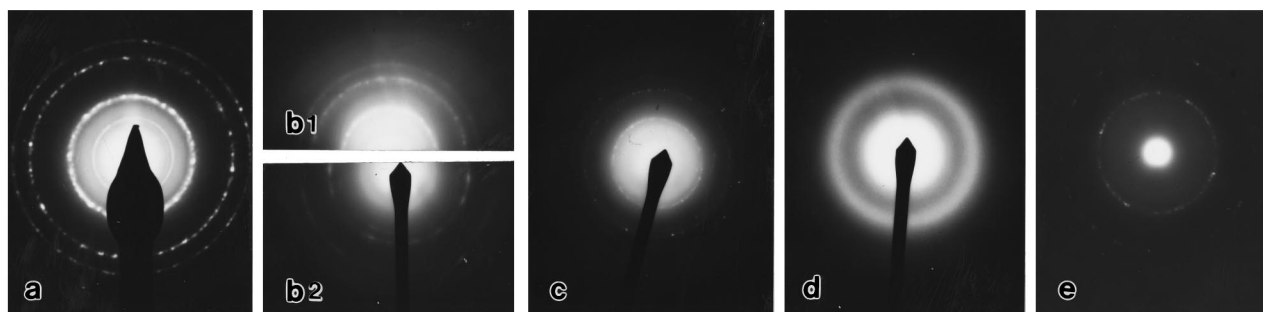


FIG. 1. SAED patterns of Si nanowires with different doping doses of Li^+ ions: (a) undoped Si NWs; (b) lightly-doped; (c) heavily doped; (d) more heavily doped; and (e) Li^+ ions extracted from the state of (d).

c-Si structure [Fig. 1(c)] is found. At the more heavily doped state, the crystalline diffraction pattern disappears and diffuse diffraction halos are presented in Fig. 1(d), indicating that the crystalline structure is destroyed completely. However, the crystalline diffraction pattern indexed with the *c*-Si structure [Fig. 1(e)] is visible again when the Li^+ ions are extracted from the Si NWs.

The bonding state and chemical composition of the nanowires were determined by PEELS. The spot size of the electron probe is about 5 nm in diameter and the spectra were taken from a single nanowire. Figure 2(a) is the PEELS of undoped Si NWs. Figure 2(b) is the PEELS of Li^+ ion-doped Si NWs, which indicates the presence of Li and Si.

The HREM images in Figs. 3(a), 3(b), 3(c), and 3(d) are, respectively, correspondent to the Li^+ ion-doping state of the Si NWs as indicated in Figs. 1(b), 1(c), 1(d) and 1(e). A crystalline core and an amorphous outer layer with thickness of 3 nm can be seen in Fig. 3(a). The interplanar spacing is 0.31 nm in the core of the nanowire, which corresponds to the $\{111\}$ plane. However, the spacing of 0.32 nm is also visible at some regions. Furthermore, the amorphous layer at the outer part of the doped Si NWs is also thicker than that occurring as the surface layer in the undoped nanowires⁴ and some completely amorphous regions are also visible as indexed by the black arrows. This nonuniform lattice expansion and destruction of the crystalline structure of the Si NWs indicate a heterogeneous distribution of Li^+ ions. The HREM image in the inset of Fig. 3(a) is taken from the Li^+

ion-doped Si NWs whose diffraction pattern is shown in Fig. 1(b) (2). The interplanar spacing of the image is 0.25 nm. With increasing of the doping dose, the lattice expansion becomes more obvious and the outer amorphous region develops further towards the core of the Si NWs [Fig. 3(b)]. The amorphous layer is about 5 nm, and many regions with a crystalline structure in the core of the Si NWs are destroyed completely. The spacing of the remaining crystalline regions is about 0.32 nm. When the Si NWs are doped with a high dose of Li^+ ions, the crystalline structure is destroyed completely, and transformed into amorphous Li-Si nanowires [Fig. 3(c)].

According to the above HREM investigation, it is found that the lattice of the crystalline Si will be expanded due to the insertion of Li^+ ions. With increasing the doping dose, the Si-Si bonds are broken and at last, the crystalline nanowires transform into the amorphous phase. On the other hand, the kinetic metastable phase of Li-Si may be formed in the light doping state, and this metastable phase will disappear with the increasing of doping dose. When the Li^+ ions are extracted from the heavily doped Li-Si nanowires, the short-range ordered structure with lattice distortion will be formed again in some regions of the nanowires, as shown in Fig. 3(d).

Note that large amounts of Li^+ ions can be doped into the Si NWs. The diffusion mechanism of Li^+ ions is one such as interstitial diffusion because their small atom radius allows an easy propagation of Li^+ ions via interstitial sites in the Si NWs, even at relatively low temperature. The driving force for the diffusing comes from the electric potential gradient between the lithium foil and Si NWs, and concentration gradient of Li^+ ions. According to the experimental conditions, the magnitude of the electrical field is at least 10 000 V/cm near the surface of the Si NW electrode, which leads to the mobility of the Li^+ ions. The HREM observation indicates that the doping diffusion is not highly uniform. During the electrochemical reaction process, electric-field inhomogeneities will lead to Li^+ ion current inhomogeneities, which in turn result in a nonuniform Li^+ ion distribution. Furthermore, the inhomogeneous concentration of Li^+ ions will also cause the nonuniform diffusion of lithium ions.

Studies of random crystallization of pure amorphous silicon indicate that crystallization does not occur below the temperature of about 625 °C.⁷ However, the ordered structure in the amorphous Li^+ -doped Si NWs is formed at room temperature in the present study. Figure 4 shows the dis-

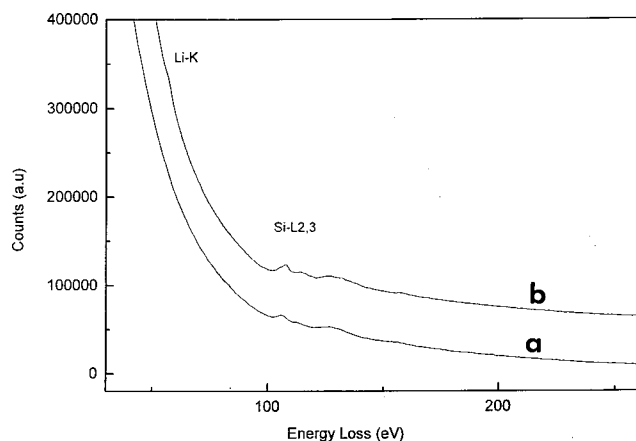


FIG. 2. PEELS taken from undoped Si NWs (a) and Li^+ -doped Si NWs (b). In curve (b), the absorption peaks at 55 and 99 eV correspond to the Li-K edge and Si- L_2 , $-L_3$ edge, respectively, which confirms the presence of lithium in Li^+ -doped Si NWs.

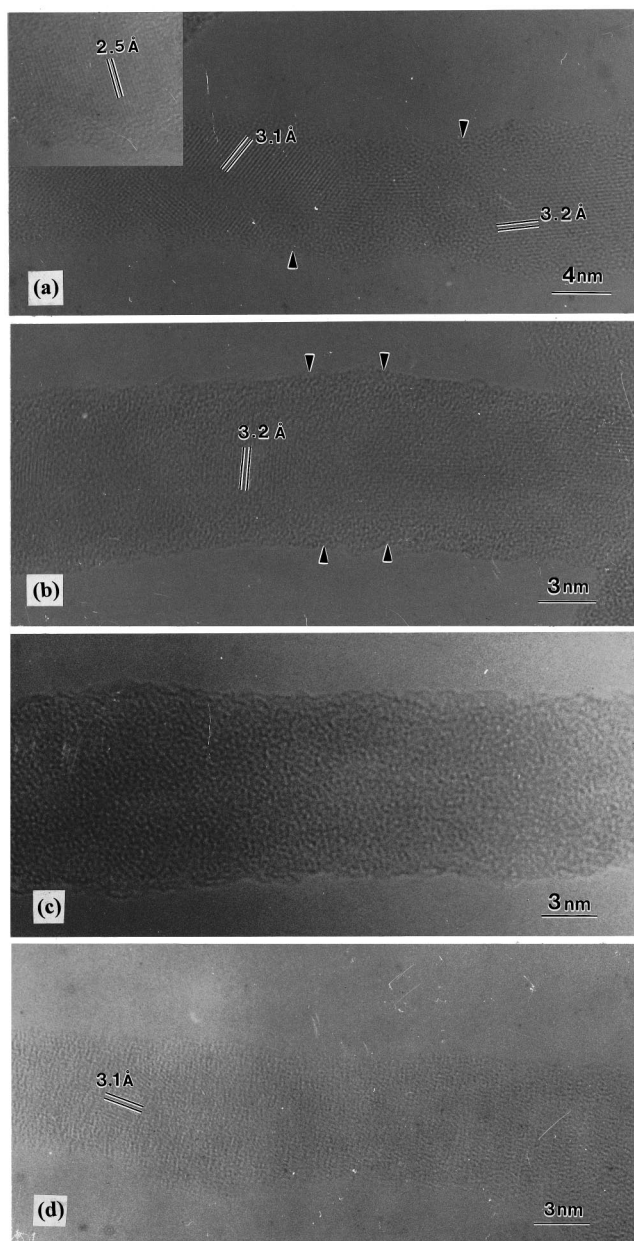


FIG. 3. HRTEM images of Si NWs at four different doping states. (a), (b), (c), and (d) show the microstructural characteristics of the doping state of (b), (c), (d), and (e) shown in Fig. 1.

charge and charge curves of the Li/Si NW cell at the first cycle. During the discharging process, the voltage of the Si NW electrode approaches the voltage of metal Li with gradual increasing of the Li^+ ions. During the charging process, the voltage of the Si NW electrode versus metal Li electrode raises up with the gradual extraction of Li^+ ions. According to this discharging/charging curve, the Si NWs have a reversible capacity of more than 1700 mAh/G Si, which is five times higher than that of current carbonaceous material in commercial lithium ion batteries (<370 mAh/g C). It is generally admitted that the energy stored in the crystalline or amorphous structure results from the local bond distortions.⁸ The insertion of Li^+ ions into Si NWs will lead to a distorted angular bond distribution. With the increasing of doping dose, the bond distortion becomes more obvious and at last destroys the silicon structure. After the

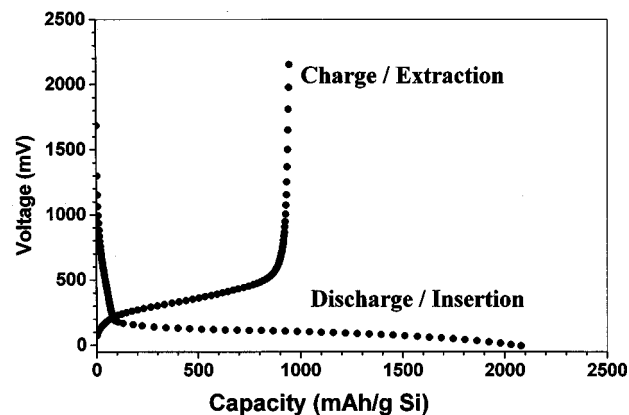


FIG. 4. Discharge (Li insertion) and charge (Li extraction) curves of a cell (–) Li/LiPF₆ in EC+DEC(1:1)/Si NWs(+) at a constant current density of 0.05 mA/cm². The voltage change of the cell is determined by the amount of Li in the Si NWs.

Li^+ ions are extracted from the Si NWs by the same method, some distorted angular bonds will be restored, the distorted and interrupted Si–Si bonds will rebond. So, the local ordered structure is formed in Li^+ -doped Si NWs.

Photoluminescence (PL) measurements of Si NWs at different doping states were performed at room temperature. A light emission center around 583 nm was observed in the undoped Si NW sample. This peak was shifted to 548 nm and its intensity was raised (about four times than that of the undoped Si NWs) at the light-doping state. The PL peak was shifted to 540 nm and the intensity was reduced at the heavily doping state. After the Li ions were extracted from the Si NWs, the PL peak was redshifted to 590 nm. This result shows that the PL peak and intensity of Li^+ -doped Si NWs are closely related to the doping dose. It is thus conjectured that the band gap of Li^+ -doped Si NWs is correlated with the doping dose. It has been shown that extent of the Si valence band depends on the number of uninterrupted Si–Si bonds.⁹ Therefore, Si NWs with different band-gap structures can be obtained by controlling the doping level.

An effective method was presented to dope Si NWs with a controlled doping level. The properties of Si NWs will be modified by controlling the voltage of chemical reaction to cause different doping levels. By analogy of this method, other elements can also be incorporated into Si NWs.

¹D. P. Yu, C. S. Lee, I. Bello, X. S. Sun, Y. H. Tang, G. W. Zhou, Z. G. Bai, Z. Zhang, and S. Q. Feng, *Solid State Commun.* **105**, 403 (1998); M. Morales and C. M. Lieber, *Science* **279**, 208 (1998).

²D. P. Yu, Z. G. Bai, J. J. Wang, Y. H. Zou, W. Qian, J. S. Fu, H. Z. Zhang, Y. Ding, G. C. Xiong, S. Q. Feng, L. P. You, and J. Xu, *Phys. Rev. B* **59**, R2498 (1999).

³J. M. Lauerhaas and M. J. Sailor, *Science* **261**, 1567 (1993); A. M. Rao, P. C. Eklund, S. Bandow, A. Thess, and R. E. Smalley, *Nature (London)* **388**, 257 (1997).

⁴G. W. Zhou, Z. Zhang, Z. G. Bai, S. Q. Feng, and D. P. Yu, *Appl. Phys. Lett.* **73**, 677 (1998).

⁵G. W. Zhou, Z. Zhang, and D. P. Yu, *J. Cryst. Growth* **197**, 129 (1998).

⁶C. J. Wen and R. A. Huggins, *J. Solid State Chem.* **37**, 271 (1981); K. Amezawa, N. Yamamoto, Y. Tomii, and Y. Ito, *J. Electrochem. Soc.* **145**, 1986 (1998).

⁷J. Roth and G. L. Olson, *Mater. Res. Soc. Symp. Proc.* **74**, 319 (1987); E. Nygren, A. P. Pogany, K. T. Short, and J. S. Williams, *Appl. Phys. Lett.* **52**, 439 (1988).

⁸R. Grigorovici and R. Manaila, *Thin Solid Films* **1**, 343 (1967).

⁹H. Bock, W. Ensslin, F. Feher, and R. Freund, *J. Am. Chem. Soc.* **98**, 668 (1976).